Accepted Manuscript

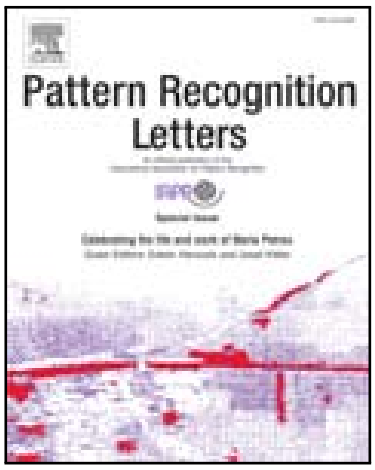

Iris Recognition using Multiscale Morphologic Features

Saiyed Umer, Bibhas Chandra Dhara, Bhabatosh Chanda

PII: S0167-8655(15)00211-1
DOI: 10.1016/j.patrec.2015.07.008
Reference: PATREC 6277

To appear in: *Pattern Recognition Letters*

Received date: 27 January 2015
Accepted date: 4 July 2015

Please cite this article as: Saiyed Umer, Bibhas Chandra Dhara, Bhabatosh Chanda, Iris Recognition using Multiscale Morphologic Features, *Pattern Recognition Letters* (2015), doi: 10.1016/j.patrec.2015.07.008

Highlights

- We present an iris recognition system with improved performance using a novel morphologic method for feature extraction.
- The iris features are represented by the sum of dissimilarity residues obtained by applying top-hat morphology operator.
- Only a part of iris image has been used for feature extraction and a SVM is used as the classifier.
- The performance of the proposed system is tested with four standard databases UPOL, MMU1, IITD, and UBIRIS.

Iris Recognition using Multiscale Morphologic Features

Saiyed Umer[a,*], Bibhas Chandra Dhara[b], Bhabatosh Chanda[a]

[a]*Electronics and Communication Sciences Unit, Indian Statistical Institute, Kolkata, India*
[b]*Department of Information Technology, Jadavpur University, Kolkata, India*

Abstract

A new set of features for personal verification and identification based on iris image is proposed in this paper. The method consists of three major components: image pre-processing, feature extraction and classification. During image pre-processing, the iris segmentation is carried out using Restricted Circular Hough transformation (RCHT). Then only two disjoint quarters of the segmented iris pattern are normalized which is used to extract features for classification purposes. Here, method for feature extraction from iris pattern is based on multiscale morphologic operator. In this approach, the iris features are represented by the sum of dissimilarity residues obtained by applying morphologic top-hat transform. For classification purposes the multi-class problems is transformed to two-class problem using dichotomy method. The performance of the proposed system is tested on four benchmark iris databases UPOL, MMU1, IITD, and UBIRIS and is compared with well known existing methods.

Keywords: Biometric, Iris recognition, Hough transform, Multiscale morphology, Toggle filter, SVM classifier

1. Introduction

Biometric refers to a person's behavioral (e.g, signature, gait, keystroke or voice) or physiological (e.g., face, iris, fingerprint or palmprint) characteristic. The physiological biometric characteristics are associated with the body parts which are generally stable, whereas behavioral biometrics are related to the behavior of the person and are relatively less stable. To authenticate a person's identity, biometric systems are advantageous compared to knowledge (e.g., password or PIN) or token (e.g., ATM card, credit card or smart card) based approaches. Iris is one of the most useful biometric traits for person identification [27] due to its high stability and unalterability. Human iris is an annular region between the pupil (black portion) and the sclera region (white portion) of an eye ball. This has complex yet regular structure that provides abundant visible texture information. This texture of the iris is unique to each individual [22]. Generally, pre-processing, normalization, feature extraction, and matching are some basic steps of an iris recognition system. However, generating feature vectors from iris images, and matching with the prototype based on some distance metric are the major tasks.

Daugman [7] [6] used integro-differentio operator to localize the iris followed by 2D Gabor filters and phase coding to obtain feature vector. Wildes [41] used Circular Hough transform for iris localization, and then constructed laplacian pyramid at four different resolutions to compute the texture feature. Finally, normalized correlation is used for authentication purposes. Lim et al. [19] exploited 2-D Harr wavelet transform to extract iris features and implemented the classifier using a modified version of competitive learning neural network. In [3], 1-D wavelet transform up to four levels was used to characterize the spatial variations of the iris, and then the features are matched using dissimilarity functions. Nabti et al. [29] too proposed a multi-resolution iris feature extraction technique. They applied a special Gabor filter bank on the normalized iris image to extract the features. Ma et al. [21] devised new spatial filters to extract iris features based on Gabor filters. The concept of wavelet packets are also applied on iris pattern to extract useful features. Yong and Han [22] used multi-scale strategy to localize the iris, and extracted eigen features based on independent component analysis. Poursaberi and Araabi [30] applied morphology operator for iris localization and then Daubechies wavelet transformation was used to extract the features.

Mathematical morphology (MM) deals directly with shape information in digital images in spatial domain [14]. It is a branch of non-linear image processing defined in terms of set theoretic operations. The main advantages of MM are the ability to extract essential structural/textural information and also the shape characteristics. MM based methods are also used in iris recognition system. De Mira Jr et al. [26] proposed iris recognition system based on unique skeleton of the iris structures using MM operators. An effective iris localization method based on mathematical morphology and Gaussian filtering is proposed by Gui and Qewei [13]. Sierra et al. [34] proposed iris localization using fuzzy mathematical morphology and neural network approach. Luo [20] determined eyelid and eyelash occlusion based on mathematical morphology and the reflection spot is detected based on thresholding.

This paper presents an iris recognition system to verify as well as to identify persons in which multiscale morphology is used to extract a new set of iris features. Here, we split the system into three components: (i) image pre-processing, (ii) feature extraction, and (iii) authentication. The pre-processing

*Corresponding author: Tel.: 033-2575-2915;
Email address: saiyedumer@gmail.com (Saiyed Umer)

component consists of iris localization and normalization. For feature extraction purpose we develop a novel feature extraction algorithm using multiscale morphology. Here multiscale top-hat transformation is used to extract structural/textural features. First, the multiscale morphologic operator is applied on normalized iris image using a line structuring element with different orientations and scales. From these processed images, residue images are obtained. Finally, these residue images are accumulated to define the feature vector. For both verification and identification, the proposed classification strategy converts the given multi-class problem to a two-class problem and SVM classifier is employed to do the classification. The rest of the paper is organized as follows. The basic principle of mathematical morphology is discussed in section 2. Proposed recognition scheme is described in section 3. Experimental results and discussions are presented in Section 4. This paper is concluded in section 5.

2. The principle of multiscale morphology

Mathematical morphology provides many powerful and important tools for processing and analysis of images. The mathematical morphologic operators treat an image as a set of pixels [28]. Thus the operations are defined as interaction between object and structuring element [15] in set theoretic terms. In digital image processing, flat structuring elements of regular geometric shape like a square or a line or a disk are most commonly used. Erosion and dilation are the most basic morphological operations. Other operations like opening and closing are various combinations of erosion and dilation. Let f and B represent a grayscale image and the domain of a flat structuring element, respectively. The erosion and dilation of f by B is defined respectively as follows

$$\textit{Erosion: } (f \ominus B)(i,j) = min\{f(i+p, j+q) \mid (p,q) \in B\} \quad (1)$$

$$\textit{Dilation: } (f \oplus B)(i,j) = max\{f(i-p, j-q) \mid (p,q) \in B\} \quad (2)$$

For extracting features or objects of given shape from an image, the shape and size of the structuring element B play a crucial role. The scheme of morphological operations using structuring element (say, tB) of same shape but of varying scales (t) is termed as multiscale morphology. Multiscale opening and closing operations are defined using eqs. (1) and (2), as

$$\textit{Opening: } (f \circ tB)(i,j) = ((f \ominus tB) \oplus tB)(i,j) \quad (3)$$

$$\textit{Closing: } (f \bullet tB)(i,j) = ((f \oplus tB) \ominus tB)(i,j) \quad (4)$$

where tB is obtained by dilating $(t-1)B$ by B and can be written as

$$tB = \underbrace{B \oplus B \oplus \cdots \oplus B}_{(t-1)times} \quad (5)$$

If $t = 0$, then $tB = \{0\,,\,0\}$ and $f \circ 0B = f$. Similarly $f \bullet 0B = f$. Eq. (5) defines a sequence of multiscale structuring elements of same shape and increasing sizes. Using eqs. (3), (4) and (5), relative bright and dark top-hat transformations are defined as

$$\textit{Bright top-hat: } W_{s,t} = (f \circ sB) - (f \circ tB) \quad (6)$$

$$\textit{Dark top-hat: } D_{s,t} = (f \bullet tB) - (f \bullet sB) \quad (7)$$

where $t \in \{1, 2, \cdots, m\}$, $s \in \{0, 1, \cdots, t-1\}$ for some value of m. For $s = 0$, we may define top-hat transformation as

$$W_t = f - (f \circ tB), \quad where \quad t = 1, 2, \cdots, m \quad (8)$$

$$D_t = (f \bullet tB) - f, \quad where \quad t = 1, 2, \cdots, m \quad (9)$$

Thus we can write

$$W_{s,t} = W_t - W_s \quad (10)$$

$$D_{s,t} = D_t - D_s \quad (11)$$

for $s < t$. The top-hat transform may be used to extract texture feature through multiscale morphology [28]. It relies on the fact that open (resp. close) operation removes bright (resp. dark) features that cannot fit in the structuring element. Since, open (resp. close) is an anti-extensive (resp. extensive) operation, by subtracting the opened image from the original one, the bright features are obtained from an image. Similarly, subtracting the original image from the closed image dark features are obtained.

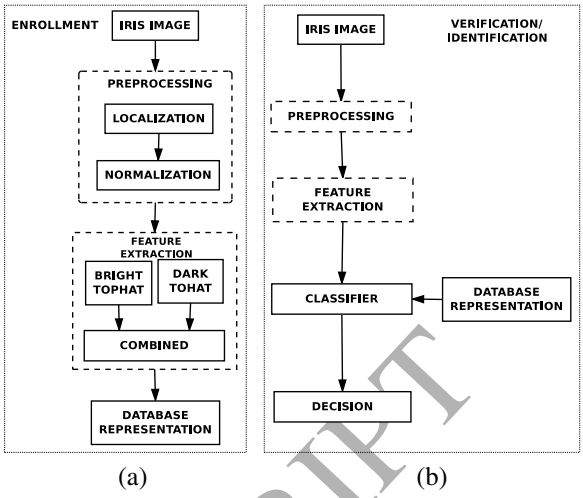

Figure 1: An overview of proposed approach: (a) Block diagram of the system (off-line) where data flow in pre-processing and feature extraction blocks are used to form representative database, (b) Block diagram of the system (on-line).

3. Proposed approach

An overview of the proposed system is shown in Fig. 1, and its flow of processing is as follows. In the pre-processing stage, we first localize the iris, i.e., the portion of the image to be actually used in classification. Then, the localized portion is normalized to facilitate the feature extraction. Normalized image is sharpened by a suitable morphological filter to highlight the texture of the iris image. Then, bright and dark top-hat transformations at different scale are computed on normalized iris image which further gives residual bright and dark details.

Then these residuals are used to form the feature vector for the iris image. Finally, support vector machine is employed as a classifier to authenticate the person whose iris image is under consideration. Brief description of each step follows.

3.1. Iris pre-processing

In this step we localize the iris region of the given eye image. Then detected iris region is normalized and sharpened. To localize the iris region we find the edge points which may not be connected to give close contours or not even circular as an iris boundary should be. So on these edge points we apply Restricted Circular Hough transform (RCHT) [39] to locate both inner (pupil-iris) and outer (iris-sclera) boundaries of iris region. The RCHT method reduces the search space and consequently the computation time of the Circular Hough transform (CHT).

3.2. Restricted Circular Hough transform (RCHT)

In basic Circular Hough transform (CHT) a 3D accumulator cell (α, β, r) is incremented for a given edge pixel (x, y) in an image as

$$r = \sqrt{(x-\alpha)^2 + (y-\beta)^2} \tag{12}$$

for all α and all β, where (α, β) is the assumed centre of the circle and r is the radius. Finally, considering all the pixels in the image, the accumulator cell with maximum value marks the centre and radius of the circle. Eq. (12) suggests that accumulator cells may be represented as a quadratic surface with one maxima in (α, β, r) space. RCHT implicitly assumes that the cell with maximum accumulated number corresponds to maxima of the surface and the accumulated number monotonically reduces in all directions. The method starts with an initial guess (α, β) for the centre, and the cells of the accumulator are incremented for all edge pixels of the image for that centre. Maximum accumulator value is noted. Then some symmetrically distributed positions at distance d from and around (α, β) are identified, and same operations are performed at these points considering them as plausible centres. The centre, for which we get maximum accumulated value over all these points, becomes the new centre and repeat the steps. Now if the new centre is same as the current centre, we reduce the distance d by 1 and repeat the process. This continues until convergence, i.e., d becomes zero. Thus RCHT becomes efficient by applying CHT at only a few potential points, i.e., (α, β). Note that mean position of the edge pixels in the boundary image is taken as the initial guess for the centre.

An example is shown in Fig 2 with $d = 3$ for illustration. Here the positions labeled by '1' are additional search positions with *cen* as the initial guess for the centre. By applying CHT at these points we find c_1 as new guessed centre, which gives new search positions labeled by '2' at $d = 3$. Proceeding similar way, we get c_2, c_3 and c_4 as possible centres in sequential order. Now considering c_4 as current center, the points labeled by '5' are marked as new search positions at $d = 3$. Now applying CHT at these points gives the same point c_4 as best possible centre. So eight new search positions labeled by '6' are marked at $d = 2$. The iteration continues with $d = 1$ and still c_4 remains the best possible centre. Thus it is considered as the final center.

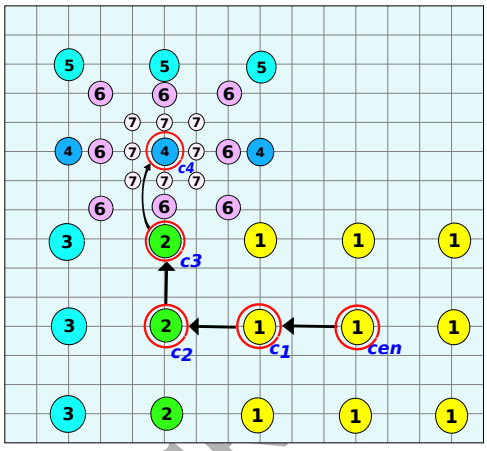

Figure 2: RCHT method illustration.

3.3. Localization

At first we analyze the histogram of the original eye image, I. Since pupil is the darkest region of the eyeball, so, in the gray-level histogram of I, this region corresponds to the peak at the lowest gray-level, and the intensity values in the vicinity of this peak or mode represent the pupil region. So by thresholding at the valley point greater than but nearest to this mode, the original image is converted to a binary image. Further this binary image is cleaned by removing small components using morphological area filter to get the image I_B. Then RCHT is applied on the boundary points in I_B to get the center and radius of the inner boundary of iris region.

In outer boundary detection process, a smooth eye image I is considered. We detect high intensity change between neighboring pixels both along horizontal or vertical direction from the center of inner boundary. Suppose d_{hl}, d_{hr}, d_{vl} and d_{vr} are the distance of these high intensity variation points from the said centre, and D is the maximum among them. So to detect the outer boundary of the iris region, we consider a square area of side $2D$ centering the inner boundary centre. Then applying RCHT on the edge pixels within this square, the circular outer contour of iris region is obtained. The localized iris region of the eye image bounded by its inner and outer boundaries are shown in Fig. 3(a). It is noted that often lower and upper portions of iris are occluded by eyelid and eyelashes. So, in the normalization process we exclude upper and lower portion of the iris region and consider only two quadrants (say, Q_1 and Q_2) as shown in Fig. 3(b).

3.4. Normalization

To normalize the image, in this paper, Daugmans Rubber sheet model [24] is applied on the selected iris region. This Rubber sheet model may be described as

$$I(x(r,\theta), y(r,\theta)) \rightarrow I_p(r,\theta) \tag{13}$$

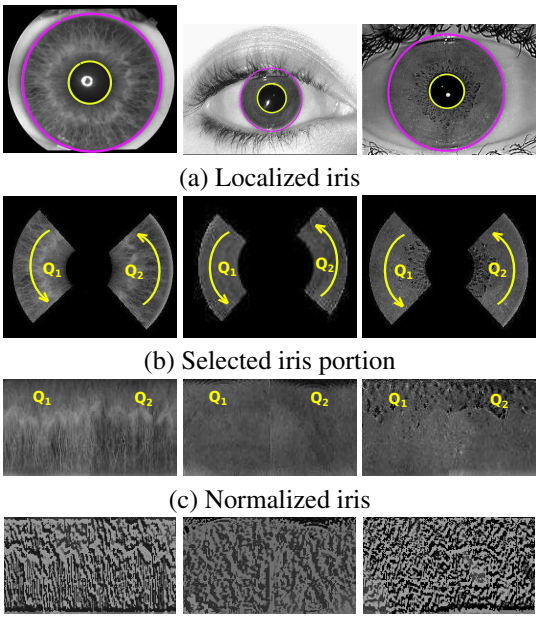

(a) Localized iris

(b) Selected iris portion

(c) Normalized iris

(d) Enhanced normalized iris

Figure 3: Illustration of iris preprocessing.

where $x(r,\theta) = (1-r)\alpha_p(\theta) + r\alpha_i(\theta)$ and $y(r,\theta) = (1-r)\beta_p(\theta) + r\beta_i(\theta)$. $I(x\ ,\ y)$ is the iris region image, $(x\ ,\ y)$ is the original Cartesian coordinates, $(r\ ,\ \theta)$ is the corresponding normalized polar coordinates, and $(\alpha_p\ ,\ \beta_p)$ and $(\alpha_i\ ,\ \beta_i)$ are the coordinates of the centers of pupil and iris, respectively. The normalized images of Fig. 3(b) are shown in Fig. 3(c).

3.5. Image sharpening using toggle filter

Iris image, in general, is a low contrast image with significant blurring in its imaged structure. Toggle filter is a morphologic tool, which may be used to sharpen the edges in the image. Mathematically toggle filter is defined using two basic morphologic operators (i.e dilation and erosion) as follows [23]

$$f_{toggle}(i,j) = \begin{cases} (f\ominus B)(i,j) \ \ if\ (f\oplus B)(i,j) - f(i,j) > f(i,j) - (f\ominus B)(i,j) \\ (f\oplus B)(i,j) \ \ if\ (f\oplus B)(i,j) - f(i,j) < f(i,j) - (f\ominus B)(i,j) \\ f(i,j) \ \ otherwise. \end{cases} \quad (13)$$

Here, the gray value of pixel in the enhanced image is obtained from the results of dilation, erosion or the original value depending on the closeness of the value. The toggle filter may be applied iteratively on the image to get sharper image. The result of toggle filter (on Fig. 3(c)) are shown in Fig. 3(d).

3.6. Feature extraction

In the pervious section, we have defined $W_{s,t}$ (*Bright* top-hat) and $D_{s,t}$ (*Dark* top-hat) by eqs. (6) and (7), respectively. In this work, to extract the texture features from the iris image (I) we consider the structuring element (B) at different scales (t) and at different orientations (θ). Let $tB(\theta)$ denotes the configuration of B at scale t with orientation θ. Then, eqs. (6) and (7) can be written as

$$W_{s,t,\theta} = I \circ sB(\theta) - I \circ tB(\theta) \quad (14)$$

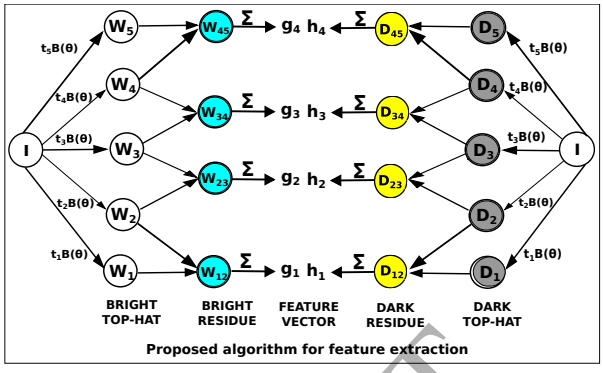

Figure 4: An example of proposed feature extraction approach for image I with structuring element B at orientation θ and at scales t_1, t_2, t_3, t_4 and t_5 to obtain features $\{g_1,\ g_2,\ g_3,\ g_4,\ h_1,\ h_2,\ h_3,\ h_4\}$.

$$D_{s,t,\theta} = I \bullet tB(\theta) - I \bullet sB(\theta) \quad (15)$$

where $t \in \{1,2,\cdots,m\}$, $s \in \{0,\cdots,t-1\}$ for some value of m. That means we consider the difference between two opened versions (or two closed versions) of the normalized image at different scales. Here, we consider difference between two successive scales. The features are extracted from normalized image as follows.

The input parameters are m and n for line structuring elements, where m is the upper limit of the scale and n represents the number of orientations. The orientation of structuring element varies from [0° - 180°). Thus, size of the feature vector (F) becomes $2\times(m-1)\times n$. Fig 4 shows an example of feature extraction technique at orientation θ and at five different scales t_1, t_2, t_3, t_4 and t_5. Eqs. (14) and (15) are applied on normalized iris image I with line SE of orientation θ and scales t_1, t_2, t_3, t_4 and t_5 which gives bright residues W_{12}, W_{23}, W_{34}, W_{45} and dark residues D_{12}, D_{23}, D_{34}, D_{45}. The bright and dark residues are aggregated individually at each scale to compute feature g_1, g_2, $\cdots$ and h_1, h_2, $\cdots$ respectively i.e. $g_i = \frac{1}{n_1 n_2}\sum_{(x,y)} W_{i,i+1}(x,y)$ and $h_i = \frac{1}{n_1 n_2}\sum_{(x,y)} D_{i,i+1}(x,y)$, where $n_1 \times n_2$ is size of the image I.

3.7. Conversion to two-class problem

For each iris image I, a feature vector F is generated using above feature extraction algorithm. These feature vectors are used to design a two-class classifier which should be able to both verify and identify a subject (person).

Conventionally during identification the system recognizes an individual by comparing it with all the templates of the subjects in the database, whereas during verification the system has to either accept or reject the claimed identity of an individual with a subject by comparing the feature vectors of these two individuals only. In this experiment, we have, say, N subjects and each subject has p number of samples. Usually, N is large, and designing a classifier for such a large number of classes seems to be difficult. To solve this problem we convert multi-class problem to a two-class problem using the dichotomy model [42]. A major advantage of the two-class approach is that even the subject, whose specimens were not

used during the training, can be identified by the system. Another advantage is that the classifier need not be retrained every time a new subject is introduced in the system. To simply understand the two-class approach, we consider N subjects $\{S_1, S_2, \cdots, S_N\}$ where each subject has p samples. For designing the classifier we first generate the feature vectors F for all samples of all subjects. Here we adopt leave-one-out classification strategy to build the system. So we set aside one sample of each subject as test sample and use rest $p-1$ samples to train the classifier. We compute mean vector V_i over $p-1$ training samples of the subject S_i. This V_i is called as the template or prototype or representative of the i-th class and is included in that class. Then from two vectors F_i and F_j we compute a difference vector $U_{i,j}$ such that its k-th element is the absolute difference between k-th elements of F_i and F_j, i.e., $U_{i,j}(k) = |F_i(k) - F_j(k)|$.

If F_i and F_j are taken from the samples of same subject, we consider $U_{i,j}$ as intra-class difference vector, and its collection $\{U_{i,j}\}$ is denoted by V_{intra}. On the other hand, if F_i and F_j are actually prototypes V_i and V_j of the i-th and j-th subjects respectively, $U_{i,j}$ is considered as inter-class difference vector and its collection forms a set V_{inter}. So we get $\binom{p}{2} \times N$ number of intra-class difference vectors and $\binom{N}{2}$ number of inter-class difference vectors. Thus our two-class classification strategy consider 'inter' (different subjects) and 'intra' (same subject) as two classes. Hence, various subsets of V_{intra} and V_{inter} of difference vectors are used for training and validation purpose in this experiment, and not the collection of raw feature vectors F_is directly.

4. Experimental results and discussions

4.1. Databases used

To evaluate the performance of the proposed method, we use four benchmark iris databases, namely, UPOL [9], MMU1 [1], IITD [18] and UBIRIS [31]. UPOL iris database contains 64 subjects and each subject has 6 (3 left (L) and 3 right (R)) eye images. The MMU1 database has 45 subjects and each subject has 10 (5 L and 5 R) eye images. The iris part in many of the images of MMU1 database suffer from severe obstructions by eyelids/eyelashes, specular reflection, nonlinear deformation, low contrast and illumination changes. The IIT Delhi database contains 224 subjects and each subject has 10 eye images (without mentioning L or R). We have manually grouped the images of each subject of this database into two subsets L and R with 5 images in each. The database of UBIRIS is composed of 1877 images taken in two sessions from 241 subjects. The images captured in the first session are of good quality, whereas the images captured in the second session suffer from irregularities in contrast, reflection, luminosity and focus [40]. For our experimentation, we select 1205 images of first session from 241 subjects with each having 5 L images.

4.2. Results and discussions

We have implemented the iris recognition system in MATLAB on fedora O/S of version 14.0 with a Intel Core i3 processor. In this paper, the recognition system is built based on SVM classifier using intra and inter-class difference vectors. The description of iris databases along with their V_{intra} and V_{inter} class vectors used in this experiment are summarized in Table 1. To implement the recognition system, LIBSVM package [5] based on RBF-kernel using leave-one-out cross validation is employed. Finally, iris recognition systems are built using SVM classifier for both L and R iris separately, and the outputs of these classifiers are fused to develop a person authentication system.

Table 1: Intra-inter class vectors for Iris databases.

Database	UPOL	MMU1	IITD	UBIRIS
Subjects	64	45	224	241
Samples/ Subject	3 L & 3 R	5 L & 5 R	5 L & 5 R	5 L
V_{intra}	$64\times\binom{3}{2}$	$45\times\binom{5}{2}$	$224\times\binom{5}{2}$	$241\times\binom{5}{2}$
V_{inter}	$\binom{64}{2}$	$\binom{45}{2}$	$\binom{224}{2}$	$\binom{241}{2}$
Image Size	768×576	320×280	320×240	800×600

In this work, we have used two disjoint parts of the iris region, and these form a normalized image of size 100×180 pixels (shown in Fig. 3(c)). Usually in various applications of mathematical morphologic operators we take regular geometric shapes like circle, square, rectangle, line etc. as structuring elements. Since linear pattern dominates in iris texture, in this experiment we use a *line* of length equal to 5 pixels as the structuring element B (i.e., at scale $t = 1$). To extract oriented linear pattern in iris as texture feature, different structuring elements are used by scaling and rotating this line B. Scale t varies from 1 to 10 and orientation $\theta \in \{0°, 5°, \cdots, 175°\}$. So the size of feature vector is $(2\times9\times36)$=648. We have used normalized iris image I_{Nor} and enhanced normalized (toggle-filtered) iris image I_{Enor} to compute the feature vector separately to study the effect of enhancement on recognition. Thus we generate two different feature vector sets of an input image. Let us denote the feature vector of first type as F_{Nor} and the feature vector of the second type as F_{Enor}.

4.2.1. Verification accuracy

During verification, we authenticate the test sample by finding the similarity score (between test sample and the subject enrolled in the database whose identity is claimed). Our method forms the difference vector of the test vector and database vector, and then this difference vector is classified as 'intra' or 'inter'. In the former case the claimed identity is verified, and it is rejected in the latter case. Since UPOL, MMU1, and IITD databases have left and right iris images for each subject, we verify with respect to left iris and right iris separately and then fuse by OR-ing (decision level) to arrive at the final decision. The verification performances for UPOL, MMU1, IITD, and UBIRIS databases are shown in Table 2 using F_{Nor} and F_{Enor} features respectively. The Table reveals that verification rate for enhanced vector F_{Enor} is much higher than that of unenhanced vector F_{Nor}.

Table 2: The Results of verification rate (%) for Iris database.

Database	F_{Nor}			F_{Enor}		
	L	R	F	L	R	F
UPOL	89.06	84.38	98.43	100	100	100
MMU1	88.89	100	100	97.78	100	100
IITD	90.81	95.00	99.10	98.12	98.23	99.55
UBIRIS	91.56			98.34		

4.2.2. *Identification accuracy*

Identification or recognition of test sample is based on N different scores (dissimilarity) obtained by comparing the test sample with each of the N different representatives of the subjects enrolled in the database as described in previous section. Then this N scores are arranged in ascending order and a rank is assigned to each sorted score. The subject with *rank* 1 is declared as the identity of the test sample if the score satisfies a tolerable limit. The *rank* 1 accuracy for both L and R iris images are obtained separately, and then these ranks are fused using different rank level fusion techniques [17], namely Highest ranking, Borda count, and Logistic regression. Out of these rank level fusion techniques, Borda count achieves highest recognition score for these four iris image databases. Table 3 shows *rank 1* identification rate (%) for four databases using both F_{Nor} and F_{Enor} features. The table shows that F_{Enor} feature vector achieves better performance compared to F_{Nor}. Hence, from now we will use feature vector of enhanced image only.

Table 3: The Results of *rank*1 identification rate (%) for Iris database.

Database	F_{Nor}			F_{Enor}		
	L	R	F	L	R	F
UPOL	87.50	84.38	90.63	100	99.48	100
MMU1	88.88	100	96.88	97.77	100	99.55
IITD	85.71	92.41	87.94	97.75	97.05	98.37
UBIRIS	85.40			97.51		

The performance evaluation for verification system is done by constructing ROC (Receiver Operating Characteristic) curve [4] [12] with high AUC (Area Under Curve). It is explained by a diagnostic test system that AUC with values between 0.9 and 1.0 may be considered excellent [37]. ROC curves using F_{Enor} for different iris databases are shown in Fig. 5(a), which reflects that the performance of the system (the said features in conjunction with SVM classifier) is quite good. For performance evaluation of the identification system, CMC (Cumulative Match Curve) [4] is analyzed for different possible ranks. Accordingly a plot of probability of correct identification versus rank is shown in Fig. 5(b). In both the figures, fused results are shown for UPOL, MMU1 and IITD databases.

4.2.3. *Comparative study*

Upper and lower iris portions of the eye are often occluded by eyelid and eyelashes. For example, we have manually checked that about 85-87% of iris samples of MMU1, IITD and UBIRIS databases are partially occluded by eyelid and eyelashes. So before feature extraction, the occluded portion of those iris samples has to be segmented out by some costly and complicated method, or we have to use some derogatory features coming from these occluded portions, which will affect the performance of the system. To resolve this problem here we simply discard lower and upper quarters of iris region instead of applying costly segmentation algorithm. To see the effect of pruning of iris region we have applied the proposed method on the entire iris region as well as on the two quarters as stated above. The results are summarized in Table 4. This table reveals that when there is no occlusion (in case of UPOL database) the performance using whole iris region and that using two quarters are same. However, when there are occlusions the performance using whole region is less than that using two quarters, because of presence of derogatory features in the former case. Hence, it may be inferred that using only two quarters of the iris region does not reduces the accuracy, but on the other hand, increases it in case of occlusion. Secondly, this scheme reduces computational time.

Table 4: Comparison of results (accuracy in %) for F_{Enor} features computed over (i) whole and (ii) two quadrants of iris region.

Database	Over whole region				Over two quadrants			
	Verification		Identification		Verification		Identification	
	L	R	L	R	L	R	L	R
UPOL	100	100	100	100	100	100	100	99.48
MMU1	88.00	100	88.00	100	97.78	100	97.77	100
IITD	91.32	93.15	89.73	90.62	98.12	98.23	97.75	97.05
UBIRIS	90.63		90.62		98.34		97.51	

4.2.4. *Comparison with other methods*

To compare the proposed method with the existing algorithms, we use F_{Enor} feature vectors. The results (i.e. accuracy) of competitive methods along with ours are shown in Table 5. Note that we have quoted the results of existing methods from the respective articles. The system protocol (feature extraction, training-testing protocol and matching) of those methods are given in Table 6. In our case Prop_{avg} (average accuracy for L and R iris) and Prop_{fusion} (fused accuracy for L and R iris) are reported. For all the methods we have presented percentage accuracy of true positive (CRR) for identification and EER for verification. From Table 5 we see that performance of our method on UPOL database is comparable with Demirel et al. [8] and Ross et al. [33] and better than Ahamed et al. [2]. For MMU1 database our performance is superior to Masood et al. [25], Rahulkar et al [32], and Harjoko et al. [16]. Note that Masood et al. [25] and Harjoko et al. [16] developed the system for both identification and verification, whereas Rahulkar et al. [32] developed the system for verification only.

For IITD iris database, Zhou et al. [43] and Kumar et al. [18] have much inferior performances than our proposed method. Rahulkar et al. [32] and Elgamal et al. [10] too show good performances but they have presented their results using very small number of subjects as compared to the proposed method.

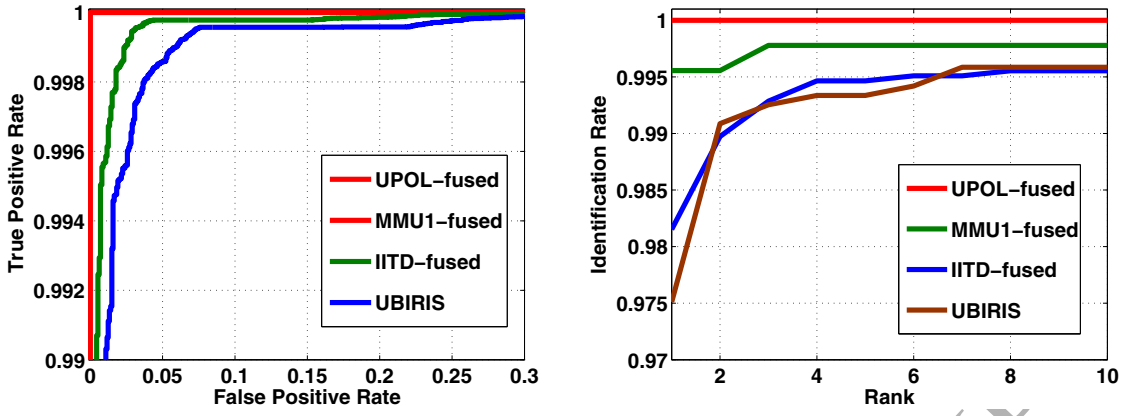

(a) (b)

Figure 5: (a) ROC and (b) CMC curves for iris databases using proposed F_{Enor} feature.

Table 5: Comparison of performance for UPOL, MMU1, IITD and UBIRIS database.

Database	Methods	Subject	CRR(%)	EER(%)
UPOL	Ahamed et al. [2]	64	97.80	0.040
	Demirel et al. [8]		100	0.000
	Ross et al. [33]		100	0.000
	Prop$_{avg}$		99.74	0.008
	Prop$_{fusion}$		100	0.005
MMU1	Harjoko et al. [16]	45	82.90	0.280
	Masood et al. [25]		95.90	0.040
	Rahulkar et al. [32]		–	1.880
	Prop$_{avg}$		98.89	0.009
	Prop$_{fusion}$		99.55	0.004
IITD	Elgamal et al. [10]	80	99.50	0.040
	Kumar et al. [18]	224	–	2.590
	Rahulkar et al. [32]	90	–	0.150
	Zhou et al. [43]	224	–	0.530
	Prop$_{avg}$	224	97.40	0.015
	Prop$_{fusion}$	224	98.37	0.007
UBIRIS	Erbilek et al. [11]	80	95.83	–
	Rahulkar et al. [32]	90	–	0.490
	Sundaram et al. [35]	190	97.00	–
	Tallapragada et al. [36]	100	99.60	–
	Tsai et al. [38]	80	97.20	7.800
	Prop	241	97.51	0.011

For UBIRIS database we see that Tsai el al. [38], Sundaram et al. [35] and Erbilek et al. [11] show marginally poor performance than the proposed method. Note that Erbilek et al. [11], Rahulkar et al. [32] and Tsai el al. [38] used very less number of subjects. Tallapragada et al. [36] have good identification performance but have used only 100 subjects, which is far less than the number of subjects used by the proposed method to report the performance.

Considering both identification and verification task and also considering the size and variety of dataset used in this experiment, the proposed method exhibits significantly superior performance compared to recently reported and well known methods. The average execution time of the proposed system is shown in Table 7. Here we have used four different databases and the images size in different databases are different, so the computational cost for iris pre-processing task is different for different databases. However, the size of normalized iris image is same for each database, so the execution time for feature extraction and authentication are same.

Table 7: Average execution time of the proposed system.

Iris Database	Original image size	Pre-processing	Feature extraction	Verification	Total (in s)
UPOL	768 × 576	0.89	0.52	0.01	1.42
MMU1	320 × 240	0.41			0.94
IITD	320 × 240	0.65			1.18
UBIRIS	800 × 600	0.92			1.45

5. Conclusion

In this paper, we present an iris recognition system with improved performance using a novel morphologic method for feature extraction. The proposed system is able to verify as well as identify the subjects efficiently. Compared to existing methods, the proposed system shows better performance. In this paper, we have adopted a fast method for iris localization. Second, only a part of iris image (to avoid occlusion problem) is used for authentication. Finally, multiscale morphologic features are extracted from sharpened segmented iris image and a SVM is used as the classifier. In future, we plan to investigate a method for combining more modalities and fusion techniques to build better multimodal biometric system.

References

[1] , . Multimedia university iris database [online]. Available:http://pesona.mmu.edu.my/ ccteo/ .

[2] Ahamed, A., Bhuiyan, M.I.H., 2012. Low complexity iris recognition using curvelet transform, in: IEEE Proc. ICIEV, pp. 548–553.

Table 6: Comparison of existing iris recognition algorithms and experimental protocols with the proposed method.

Methods	Feature	Training-testing protocol	Matching/classifier
Ahamed et al. [2]	Curvelet transform	leave-one-out	Correlation coefficient
Demirel et al. [8]	Different color space histograms	Varying sets for training & testing	Cross correlation
Ross et al. [33]	Complex steerable pyramid	Varying sets for training & testing	Classification + Fusion
Harjoko et al. [16]	Coiflet wavelet transform	3 samples for training & 2 for testing	Minimum Hamming distance
Masood et al. [25]	Haar, Symlet & Biorthogonal	3 samples for training & 2 for testing	Average absolute difference
Rahulkar et al. [32]	Triplet half-band filter bank	2 samples for training & 3 for testing	Post classifier: k-out-of-n
Elgamal et al. [10]	DWT + PCA	2/3 for training and 1/3 for testing	k-Nearest Neighbour
Kumar et al. [18]	Haar wavelet + Log-Gabor filter	Varying sets for training & testing	Minimum Hamming distance+fusion
Zhou et al. [44]	Radon transform	–	Minimum matching distance+fusion
Erbilek et al. [11]	Holistic & Subpattern-based features	2 samples for training & 3 for testing	Manhattan distance measure
Sundaram et al. [35]	GLCM based Haralick features	3 samples for training & 2 for testing	Probabilistic neural network
Tallapragada et al. [36]	Gabor features with kernel Fisher	–	SVM and HMM classifier
Tsai et al. [38]	Gabor filters	3 samples for training & 2 for testing	Possibilistic fuzzy matching strategy
Proposed	Morphologic features	leave-one-out	SVM + fusion

[3] Boles, W.W., Boashash, B., 1998. A human identification technique using images of the iris and wavelet transform. IEEE Trans. Signal Processing 46, 1185–1188.
[4] Bolle, R.M., Connell, J.H., Pankanti, S., Ratha, N.K., Senior, A.W., 2005. The relation between the roc curve and the cmc, in: IEEE Proc., pp. 15–20.
[5] Chang, C.C., Lin, C.J., 2011. Libsvm: a library for support vector machines. ACM Trans. TIST. 2, 27.
[6] Daugman, J., 2003. The importance of being random: statistical principles of iris recognition. Elsevier J. PR. 36, 279–291.
[7] Daugman, J.G., 1993. High confidence visual recognition of persons by a test of statistical independence. IEEE Trans. PAMI. 15, 1148–1161.
[8] Demirel, H., Anbarjafari, G., 2008. Iris recognition system using combined histogram statistics, in: IEEE Proc. ISCIS, pp. 1–4.
[9] Dobes, M., Machala, L., 2007. Iris database. Palacky University in Olomouc, Czech Republic, http://www. inf. upol. cz/iris .
[10] Elgamal, M., Al-Biqami, N., . An efficient feature extraction method for iris recognition based on wavelet transformation .
[11] Erbilek, M., Toygar, O., 2009. Recognizing partially occluded irises using subpattern-based approaches, in: IEEE Proc. ISCIS, pp. 606–610.
[12] Fawcett, T., 2006. An introduction to roc analysis. Elsevier J. Pattern recognition letters 27, 861–874.
[13] Gui, F., Qiwei, L., 2007. Iris localization scheme based on morphology and gaussian filtering, in: IEEE Proc. SITIS, pp. 798–803.
[14] Haralick, R.M., Sternberg, S.R., Zhuang, X., 1987. Image analysis using mathematical morphology. IEEE Trans. PAMI. , 532–550.
[15] Haralock, R.M., Shapiro, L.G., 1991. Computer and robot vision. Addison-Wesley Longman Publishing Co., Inc.
[16] Harjoko, A., Hartati, S., Dwiyasa, H., 2009. A method for iris recognition based on 1d coiflet wavelet. world academy of science, engineering and technology 56, 126–129.
[17] Ho, T.K., Hull, J.J., Srihari, S.N., 1994. Decision combination in multiple classifier systems. Pattern Analysis and Machine Intelligence, IEEE Transactions on 16, 66–75.
[18] Kumar, A., Passi, A., 2010. Comparison and combination of iris matchers for reliable personal authentication. Elsevier J. Pattern recognition 43, 1016–1026.
[19] Lim, S., Lee, K., Byeon, O., Kim, T., 2001. Efficient iris recognition through improvement of feature vector and classifier. ETRI J. 23, 61–70.
[20] Luo, Z., Lin, T., 2008. Detection of non-iris region in the iris recognition, in: IEEE Proc. ISCSCT, pp. 45–48.
[21] Ma, L., Tan, T., Wang, Y., Zhang, D., 2003. Personal identification based on iris texture analysis. IEEE Trans. PAMI. 25, 1519–1533.
[22] Ma, L., Wang, Y., Tan, T., 2002. Iris recognition using circular symmetric filters, in: IEEE Proc., pp. 414–417.
[23] Maragos, P., Pessoa, L.F., 1999. Morphological filtering for image enhancement and detection. analysis 13, 12.
[24] Masek, L., et al., 2003. Recognition of human iris patterns for biometric identification. Ph.D. thesis. Masters thesis, University of Western Australia.
[25] Masood, K., Javed, D., Basit, A., 2007. Iris recognition using wavelet, in: IEEE Proc. ICET, pp. 253–256.
[26] de Mira Jr, J., Neto, H.V., Neves, E.B., Schneider, F.K., 2013. Biometric-oriented iris identification based on mathematical morphology. Springer J. SPS. , 1–15.
[27] Miyazawa, K., Ito, K., Aoki, T., Kobayashi, K., Nakajima, H., 2005. An efficient iris recognition algorithm using phase-based image matching, in: IEEE Proc. ICIP, pp. II–49.
[28] Mukhopadhyay, S., Chanda, B., 2000. A multiscale morphological approach to local contrast enhancement. Elsevier J. Signal Processing 80, 685–696.
[29] Nabti, M., Bouridane, A., 2008. An effective and fast iris recognition system based on a combined multiscale feature extraction technique. Elsevier J. PR. 41, 868–879.
[30] Poursaberi, A., Araabi, B.N., 2005. A novel iris recognition system using morphological edge detector and wavelet phase features. Citeseer ICGST 5, 9–15.
[31] Proença, H., Alexandre, L.A., 2005. Ubiris: A noisy iris image database, in: Image Analysis and Processing. Springer, pp. 970–977.
[32] Rahulkar, A.D., Holambe, R.S., 2012. Half-iris feature extraction and recognition using a new class of biorthogonal triplet half-band filter bank and flexible k-out-of-n: A postclassifier. IEEE Trans. IFS. 7, 230–240.
[33] Ross, A., Sunder, M.S., 2010. Block based texture analysis for iris classification and matching, in: IEEE Proc. CVPRW, pp. 30–37.
[34] de Santos Sierra, A., Casanova, J.G., Avila, C.S., Vera, V.J., 2009. Iris segmentation based on fuzzy mathematical morphology, neural networks and ontologies, in: IEEE Proc., pp. 355–360.
[35] Sundaram, R.M., Dhara, B.C., 2011. Neural network based iris recognition system using haralick features, in: IEEE Proc. ICECT, pp. 19–23.
[36] Tallapragada, V., Rajan, E., 2012. Improved kernel-based iris recognition system in the framework of support vector machine and hidden markov model. IET image processing 6, 661–667.
[37] Tape, T.G., 2006. Interpreting diagnostic tests. University of Nebraska Medical Center, http://gim. unmc. edu/dxtests .
[38] Tsai, C.C., Lin, H.Y., Taur, J., Tao, C.W., 2012. Iris recognition using possibilistic fuzzy matching on local features. IEEE Trans. SMC. 42, 150–162.
[39] Umer, S., Dhara, B.C., Chanda, B., 2014. A fast and robust method for iris localization, in: Emerging Applications of Information Technology (EAIT), 2014 Fourth International Conference of, IEEE. pp. 262–267.
[40] Vatsa, M., Singh, R., Noore, A., 2008. Improving iris recognition performance using segmentation, quality enhancement, match score fusion, and indexing. IEEE Trans. SMC. 38, 1021–1035.
[41] Wildes, R.P., 1997. Iris recognition: an emerging biometric technology. IEEE Proc. 85, 1348–1363.
[42] Yoon, S., Choi, S.S., Cha, S.H., Lee, Y., Tappert, C.C., 2005. On the individuality of the iris biometric, in: Image analysis and recognition. Springer, pp. 1118–1124.
[43] Zhou, Y., Kumar, A., 2010a. Personal identification from iris images using localized radon transform, in: IEEE Proc. ICPR, pp. 2840–2843.
[44] Zhou, Y., Kumar, A., 2010b. Personal identification from iris images using localized radon transform, in: Pattern Recognition (ICPR), 2010 20th International Conference on, IEEE. pp. 2840–2843.